

A simple tensor network algorithm for 2d steady states

Augustine Kshetrimayum,¹ Hendrik Weimer,² and Román Orús¹

¹*Institute of Physics, Johannes Gutenberg University, 55099 Mainz, Germany*

²*Institut für Theoretische Physik, Leibniz Universität Hannover, Appelstr. 2, 30167 Hannover, Germany*

Here we present a tensor network algorithm that approximates steady-states of 2d quantum lattice dissipative systems in the thermodynamic limit. The implementation of our method is remarkably simple and efficient. We prove the validity of the approach by computing the steady states of a dissipative quantum Ising model, relevant to address controversies in dissipative systems of interacting Rydberg atoms, and benchmark our simulations with a variational algorithm based on product and correlated states. Our results support the existence of a first order transition in this model, while we find no evidence for a bistable region. We also simulate a dissipative spin-1/2 XYZ model, showing that there is no re-entrance of the ferromagnetic phase. Our method is the first 2d tensor network implementation to compute steady states in 2d quantum lattice systems.

Introduction.- Understanding the effects of dissipation in quantum many-body systems is an open challenge. When the quantum system is immersed in an environment and coupled to it, the exchange of information (i.e., energy, heat, particles...) between system and environment usually leads to *dissipation* when the environment is larger than the system. If the dissipation is Markovian (i.e., if no information flows back into the system), then the evolution is generated by a Liouvillian superoperator \mathcal{L} , and can be casted in the form of a master equation for the reduced density matrix of the quantum system. As time flows, the system dissipates, until reaching in many cases a *steady, or “dark” state*, which is the right eigenvector of \mathcal{L} with zero eigenvalue. This process is important in several contexts, e.g., understanding the decoherence of complex wavefunctions [1], quantum thermodynamics [2], engineering of topological order through dissipation [3], and driven-dissipative universal quantum computation [4]. The study of non-equilibrium quantum complex systems has boosted recently [5–9].

In this paper we present a method to approximate such steady states for 2d quantum lattice systems of infinite size (i.e., in the thermodynamic limit). Over the years, the solution to this problem has proven remarkably difficult. Our method is to be compared to alternatives in 2d such as cluster mean-field methods [10], correlated and product state variational ansatzs [11, 12], and corner-space renormalization group [13]. Importantly, none of these methods targets the truly 2d quantum correlations that are present in the problem. The method that we propose here is based on Tensor Networks (TN) [14] and is, in fact, particularly simple and efficient. Whereas TN methods have been used in the context of dissipative 1d systems [15, 16], our method is the first approach that uses truly 2d TNs to target 2d dissipation. To prove the validity of our algorithm, we compute the steady states of the dissipative 2d quantum Ising model for spin 1/2, which is of relevance for controversies concerning dissipation for interacting Rydberg atoms [11]. As we shall discuss, we compare our results with those obtained by a variational algorithm based on product and correlated

states [12]. Moreover, we also simulate a dissipative spin-1/2 XYZ model, showing that there is no re-entrance of the ferromagnetic phase, as opposed to recent cluster mean-field results [10].

Parallelism with imaginary time.- We start by considering a master equation of the form

$$\dot{\rho} = \mathcal{L}[\rho] = -i[H, \rho] + \sum_{\mu} \left(L_{\mu} \rho L_{\mu}^{\dagger} - \frac{1}{2} \{L_{\mu}^{\dagger} L_{\mu}, \rho\} \right), \quad (1)$$

where ρ is the density matrix of the system, \mathcal{L} is the Liouvillian superoperator, H the Hamiltonian of the system, and $\{L_{\mu}, L_{\mu}^{\dagger}\}$ the Lindblad operators responsible for the dissipation. Following a similar approach as in Ref.[17], we can also write the same equation in *vectorized* form using the so-called “Choi’s isomorphism”, i.e., understanding the coefficients of ρ as those of a vector $|\rho\rangle_{\sharp}$ [36] (see Fig.1(a)): $|\rho\rangle_{\sharp} = \mathcal{L}_{\sharp} |\rho\rangle_{\sharp}$, where the “vectorized” Liouvillian is given by

$$\mathcal{L}_{\sharp} \equiv -i(H \otimes \mathbb{I} - \mathbb{I} \otimes H^T) + \sum_{\mu} \left(L_{\mu} \otimes L_{\mu}^* - \frac{1}{2} L_{\mu}^{\dagger} L_{\mu} \otimes \mathbb{I} - \frac{1}{2} \mathbb{I} \otimes L_{\mu}^* L_{\mu}^T \right). \quad (2)$$

In the above equation, the symbol of tensor product \otimes separates operators acting on either the l.h.s. (ket) or the r.h.s. (bra) of ρ in its matrix form. Whenever \mathcal{L}_{\sharp} is independent of time, time evolution can be formally written as $|\rho(T)\rangle_{\sharp} = e^{T\mathcal{L}_{\sharp}} |\rho(0)\rangle_{\sharp}$, which for very large times T may yield a steady state $|\rho_s\rangle_{\sharp} \equiv \lim_{T \rightarrow \infty} |\rho(T)\rangle_{\sharp}$. It is easy to see that the state $|\rho_s\rangle_{\sharp}$ is the eigenvector of \mathcal{L}_{\sharp} corresponding to zero eigenvalue, so that $\mathcal{L}_{\sharp} |\rho_s\rangle_{\sharp} = 0$.

Next, let us consider the special but quite common case in which the Liouvillian \mathcal{L} can be decomposed as a sum of local operators. For nearest-neighbor terms, one has the generic form $\mathcal{L}[\rho] = \sum_{\langle i,j \rangle} \mathcal{L}^{[i,j]}[\rho]$, where the sum $\langle i,j \rangle$ runs over nearest-neighbors. In the “vectorized” notation (\sharp), this means that $\mathcal{L}_{\sharp} = \sum_{\langle i,j \rangle} \mathcal{L}_{\sharp}^{[i,j]}$.

The combination of the expressions above yields a parallelism with the calculation of ground states of local

Ground states	Steady states
$H = \sum_{\langle i,j \rangle} h^{[i,j]}$	$\mathcal{L}_{\#} = \sum_{\langle i,j \rangle} \mathcal{L}_{\#}^{[i,j]}$
e^{-TH}	$e^{T\mathcal{L}_{\#}}$
$ e_0\rangle$	$ \rho_s\rangle_{\#}$
$\langle e_0 H e_0\rangle = e_0$	$\# \langle \rho_s \mathcal{L}_{\#} \rho_s \rangle_{\#} = 0$
Imaginary time	Real time

TABLE I: Parallelism between the calculation of ground states by imaginary-time evolution, and the calculation of steady states by real-time evolution. On the left hand side, H is a Hamiltonian that decomposes as a sum of local terms $h^{[i,j]}$, $|e_0\rangle$ is the ground state of H with eigenvalue e_0 , and T is the imaginary time.

Hamiltonians by imaginary-time evolution, which we detail in Table I.

Computing 2d steady states.— Given the parallelism above, it is clear that one can adapt, at least in principle, the methods to compute imaginary time evolution of a pure state as generated by local Hamiltonians, to compute also the real time evolution of a mixed state as generated by local Liouvillians [37].

Inspired by the above, our method for 2d systems proceeds by representing the reduced density operator ρ by a Projected Entangled State Operator (PEPO) [14] with physical dimension d and bond dimension D , see Fig.1(b) [38]. Once vectorized, the PEPO can be understood as a Projected Entangled Pair State (PEPS) [21] of physical dimension d^2 and bond dimension D , as shown also in Fig.1(b). Next, we notice that for the case of an infinite-size 2d system, this setting is actually equivalent to that of the infinite-PEPS algorithm (iPEPS) to compute ground states of local Hamiltonians in 2d in the thermodynamic limit [22]. Thus, in principle, we can use the full machinery of iPEPS to tackle as well the problem of 2d dissipation and steady states.

There seems to be, however, one problem with this idea: unlike in imaginary-time evolution, we are now dealing with real time. In the master equation, part of the evolution is generated by a Hamiltonian H , and part by the Lindblad operators L_{μ} . The Hamiltonian part corresponds actually to a unitary ‘‘Schrödinger-like’’ evolution in real time, which typically increases the ‘‘operator-entanglement’’ in $|\rho\rangle_{\#}$, up to a point where it may be too large to handle for a TN representation (e.g., 1d MPO or 2d PEPO) with a reasonable bond dimension. In 1d this is the reason why the simulations of master equations are only valid for a finite amount of time. In 2d, simple numerical experiments indicate that in a typical simulation the growth of entanglement is even faster than in 1d.

Luckily, this is not a dead-end: if the dissipation is strong compared to the rate of entanglement growth, then the evolution drives the system into the steady state before hitting a large-entanglement region. In fact, even if there is too much entanglement for the TN, the dissi-

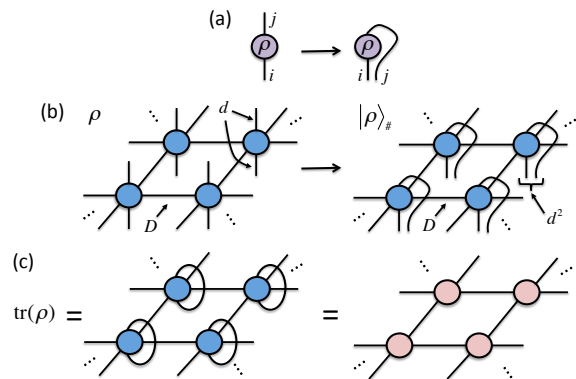


FIG. 1: [Color online] (a) TN diagram for the reduced density matrix ρ , with matrix elements ρ_i^j . The vectorization (or Choi’s isomorphism) is, simply, putting the two indices i and j together, and reshaping them into a single index $\{i, j\}$; (b) TN diagram for the PEPO representation of ρ on a 2d square lattice, with bond dimension D and physical dimension d . When vectorized, it can be understood as a PEPS for $|\rho\rangle_{\#}$ with bond dimension D and physical dimension d^2 ; (c) When computing the trace of ρ , the problem maps to the contraction of a 2d TN of tensors, quite similar to a 2d classical partition function.

ipation may still drive the evolution towards a good approximation of the correct steady state. *The main point of this paper is to show that, quite surprisingly, this is indeed the case for 2d dissipative systems* [39].

With this in mind, our algorithm just applies the iPEPS machinery to compute the time evolution in 2d with a local Liouvillian \mathcal{L} and some initial state. For the examples shown in this paper, we use the so-called *simple update* scheme [23] for the time-evolution of the PEPO, Corner Transfer Matrices (CTM) [24] for the calculation of observables [40], and random initial states. To check whether we have a good approximation of a steady state or not we compute the parameter $\Delta \equiv \# \langle \rho_s | \mathcal{L}_{\#} | \rho_s \rangle_{\#}$. For a good steady-state approximation, this parameter should be close enough to zero, since we have $\Delta = 0$ in the exact case [41]. Another quantity that we used to check the validity of the simulations is the sum of negative eigenvalues of the (numerical) reduced density matrices of the system. More precisely, we define $\epsilon_n \equiv \sum_{i|\nu_i < 0} \nu_i(\rho_n)$, where ρ_n is the reduced density matrix of n contiguous spins in the steady state and $\nu_i(\rho_n)$ its eigenvalues, with only the negative ones entering the sum. In an exact case, this quantity should be equal to zero. However, the different approximations in the method may produce a small negative part in ρ_s , which can be easily quantified in this way [42].

The computational cost of this algorithm is the one of the chosen iPEPS strategy. In our case, we work with a simple update for the evolution with a 2-site unit cell, which has a cost of $O(d^4 D^5 + d^{12} D^3)$, and Trotter time-steps $\delta t = 0.1 - 0.01$. Moreover, the CTM method for expectation values is essentially the one used to approx-

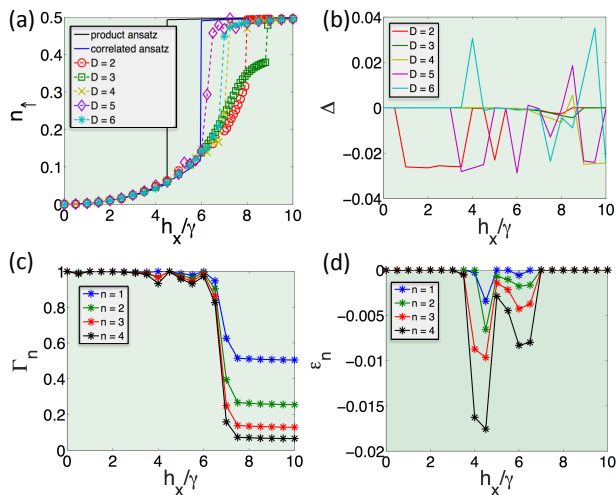


FIG. 2: [Color online] (a) spin-up density in the steady state as a function of h_x/γ for $V = 5\gamma, \gamma = 0.1$ and $h_z = 0$, as computed with our method up to $D = 6$. For comparison, we show the results obtained by the variational method from Ref.[12] with product states (black line) and correlated states (blue line); (b) Expectation value of \mathcal{L}_z in vector $|\rho_s\rangle_z$, up to $D = 6$; (c) Purity Γ_n of the reduced density matrix for a block of n contiguous spins, for $D = 6$ (other bond dimensions have similar behaviour). Spins are chosen within the 2×2 unit cell of the TN; (d) Sum of the negative eigenvalues ϵ_n of the reduced density matrix for a block of n contiguous spins, for $D = 6$ (other bond dimensions have similar behaviour). Overall, the convergence of the results can be further improved by using more accurate update schemes for the tensors throughout the time evolution.

imate classical partition functions on a 2d lattice (see Fig.1(c)), which has a cost of $O(dD^4 + \chi^2 D^4 + \chi^3 D^3)$, being χ the CTM bond dimension. The overall approach is thus remarkably efficient [43].

Results. - We first benchmark our method by simulating a dissipative spin-1/2 quantum Ising model on an infinite 2d square lattice, where dissipation pumps one of the spin states into the other. This model is of interest in the context of recent experiments with ultracold gases of Rydberg atoms [28, 29]. Moreover, the phase diagram of its steady state is still a matter of controversy. Initially, it was predicted that the model exhibits a bistable phase [30, 31], but several numerical and analytical calculations have cast doubts on this claim [11, 12, 16, 32]. In particular, a variational approach [11, 12] predicts that the bistable phase is replaced by a first order transition, which is also supported by arguments derived from a field-theoretical treatment of related models within the Keldysh formalism [32]. Furthermore, it is an open question whether the model supports an antiferromagnetic phase [11, 12, 30, 33, 34]. The master equation follows the one in Eq.(1), where the Hamiltonian part is given by $H = \frac{V}{4} \sum_{\langle i,j \rangle} \sigma_z^{[i]} \sigma_z^{[j]} + \frac{h_x}{2} \sum_i \sigma_x^{[i]} + \frac{h_z}{2} \sum_i \sigma_z^{[i]}$, with $\sigma_\alpha^{[i]}$ the α -Pauli matrix at site i , V the interaction strength,

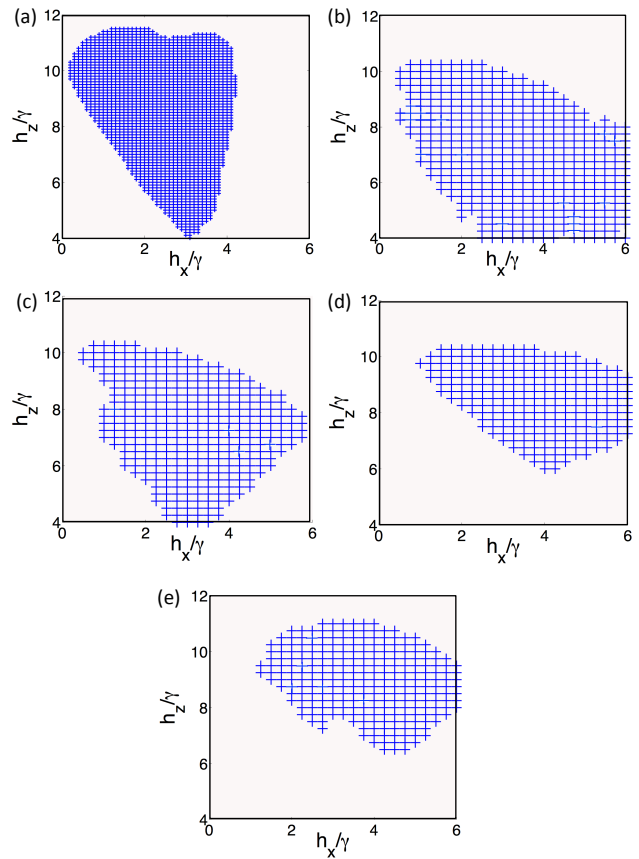


FIG. 3: [Color online] AF region (in blue) in parameter space, for $V = 5\gamma$ and $\gamma = 0.1$: (a) variational product-state ansatz from Ref.[11]; (b) TN method with $D = 2$; (c) TN method with $D = 3$; (d) TN method with $D = 4$; (e) TN method with $D = 5$. In our calculations, we see no AF phase in this region for $D = 6, 7, 8$ and 9 . Numerically, we see that the population difference drops down to $\sim 10^{-9}$ as soon as the AF disappears, whereas it is $\sim 10^{-1}$ when we observe it.

h_x, h_z the transverse and parallel fields respectively, and where the sum over $\langle i, j \rangle$ runs over nearest neighbors. The dissipative part is given by operators $L_\mu = \sqrt{\gamma} \sigma_-^{[\mu]}$, so that in this particular case μ is a site index, and where σ_- is the usual spin-lowering operator.

In our simulations, we first set $V = 5\gamma, \gamma = 0.1, h_z = 0$ in order to compare with the results in Ref.[12], which use a correlated variational ansatz with states of the form $\rho = \prod_i \rho_i + \sum_{\langle i,j \rangle} C_{ij} \prod_{k \neq i,j} \rho_k$, where ρ_i are single site density matrices and C_{ij} account for correlations. We compute the density of spins-up $n_\uparrow \equiv \sum_{i=1}^N \langle (1 + \sigma_z^{[i]}) \rangle / 2N$ (N is the system's size) as a function of h_x/γ , for which it is believed to exist a 1st order transition in the steady state from a “lattice gas” to a “lattice liquid”. This transition is clearly observed in our simulations in Fig.(2(a)), where simulations for $D = 5, 6$ agree with the correlated variational ansatz in the location of the transition point at $h_x^*/\gamma \sim 6$. In fact, as the bond dimension D in creases, we observe that there is more tendency towards agreeing

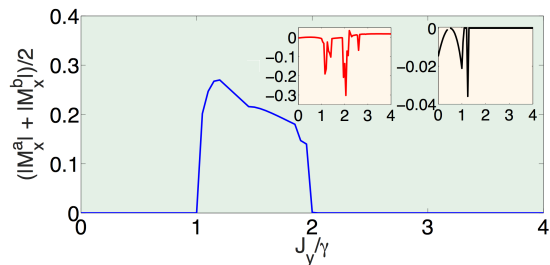


FIG. 4: [Color online] Ferromagnetic order parameter for the XYZ model, for $J_x = 0.5, J_z = 1$ and $D = 4$, as an average of $|M_x| = |\langle \sigma_x \rangle|$ over the two sites a and b in our 2d PEPO construction of ρ . We observe no re-entrance of the ferromagnetic order at large values of J_y/γ , as opposed to Ref.[10]. The left inset shows parameter Δ , and the right inset ϵ_n for 4 contiguous spins in a 2×2 plaquette. As expected, we observe larger errors around the phase transition regions. Larger bond dimensions did not change the conclusion.

with the correlated variational ansatz. Other quantities can also assess this transition, e.g., the purity of the n -site reduced density matrix $\Gamma_n \equiv \text{tr}(\rho_n)$, which we plot in Fig.(2(c)) for $D = 6$. We can see from that plot that the steady states ρ_s for low h_x/γ are quite close to a pure state (for which $\Gamma_n = 1/V^n$). To validate this simulations we computed the parameters Δ and ϵ_n introduced previously, which we show in Fig.(2(b)) and Fig.(2(d)) respectively. One can see that Δ is always quite close to zero in our simulations, being at most $|\Delta| \sim 0.03$, so that the approximated ρ_s is close to the exact steady state. Moreover, one can also see that ϵ_n is always rather small, e.g., for $D = 6$ it is at most $\epsilon_n \sim -0.017$ for the 4-site density matrix close to the transition region (similar conclusions hold for other bond dimensions). This implies that the negative contribution to the numerical reduced density matrix is quite small, and therefore does not lead to large errors. In practice, we see that ϵ_n seems to be extensive in n away from the transition region, more specifically, $\epsilon_n \sim n\epsilon_0 + O(1/n)$, with ϵ_0 very close to zero. In our simulations we always find a unique steady state, as opposed to bistability [12].

Next, we introduce non-zero values of the parallel field h_z . In some regions of the phase diagram, mean-field and correlated state variational methods predict the existence of an “antiferromagnetic” (AF) phase, where n_\uparrow attains different values between nearest neighbours in the square lattice [11]. In our simulations we have also found this antiferromagnetic region up to $D = 5$, see Fig.(3) for $V = 5\gamma, \gamma = 0.1$, where for comparison we also show the data from Ref.[11] for the variational ansatz with product states. Quite surprisingly, however, we find no AF phase for $D = 6, 7, 8$ and 9 around this region. The AF phase thus disappears for large bond dimension and for these values of the parameters. Notice that, however, this does not rule out the possibility of an AF phase appearing at some other parameter region.

Additionally, we have simulated a dissipative spin-1/2 XYZ model on an infinite 2d square lattice, with Hamiltonian $H = \sum_{\langle i,j \rangle} (J_x \sigma_x^{[i]} \sigma_x^{[j]} + J_y \sigma_y^{[i]} \sigma_y^{[j]} + J_z \sigma_z^{[i]} \sigma_z^{[j]})$, and the same jump operators $L_\mu = \sqrt{\gamma} \sigma_-^{[\mu]}$. This model has been analyzed recently by cluster mean-field and corner space renormalization methods [10, 13]. In particular, in Ref.[10], a possible re-entrance of the ferromagnetic phase at large coupling was discussed. In our simulations at large bond dimension, however, we found no signal of such an effect, see Fig.(4) for results in the regime $J_x = 0.5, J_z = 1$, and $D = 4$. Larger bond dimensions did not change this conclusion.

Conclusions and outlook. - Here we presented a simple TN method to approximate steady states for 2d quantum lattice systems of infinite size. Our approach relies on the hypothesis that the dissipative fixed-point attractor is so strong that it drives the simulation to a good approximation of the steady state even when the intermediate time-evolved states have too much entanglement for the TN representation. We benchmarked our method with dissipative Ising and XYZ models. Future applications include the engineering of topologically-ordered states by dissipation in 2d quantum lattice systems. It could also be applied to finite-temperature states, provided that a microscopic model for the coupling to the heat bath is included. Finally, it would be interesting to understand these results in the context of area-laws for rapidly mixing dissipative quantum systems [35].

A. K. and R. O. acknowledge JGU, DFG, and discussions with I. McCulloch, A. Gangat, Y.-Jer Kao, M. Rizzi, D. Porrás, J. Eisert, J. J. García-Ripoll, and C. Ciuti. H. W. acknowledges the Volkswagen Foundation, DFG SFB 1227 (DQ-mat) and SPP 1929 (GiRyd).

-
- [1] M. Schlosshauer, Rev. Mod. Phys. **76** 1267 (2005).
 - [2] S. Vinjanampathy and J. Anders, Con. Phys. **57**, 3, 1-35 (2016).
 - [3] S. Diehl *et al*, Nat. Phys. **7**, 971-977 (2011).
 - [4] F. Verstraete, M. M. Wolf and J. I. Cirac, Nat. Phys. **5**, 633-636 (2009).
 - [5] M. Hönig *et al*, Phys. Rev. A **87**, 023401 (2013).
 - [6] I. Pizorn, Phys. Rev. A **88**, 043635 (2013).
 - [7] F. W. G. Transchel, A. Milsted and T. Osborne, arXiv:1411.5546.
 - [8] A. H. Werner *et al*, Phys. Rev. Lett. **116**, 237201 (2016).
 - [9] F. Iemini *et al*, Phys. Rev. B **93**, 115113 (2016).
 - [10] J. Jin *et al*, Phys. Rev. X **6**, 031011 (2016).
 - [11] H. Weimer, Phys. Rev. A **91**, 063401 (2015).
 - [12] H. Weimer, Phys. Rev. Lett. **114**, 040402 (2015).
 - [13] R. Rota *et al*, arXiv:1609.02848.
 - [14] R. Orús, Annals of Physics **349** 117-158 (2014); J. Eisert, Modelling and Sim. **3**, 520 (2013); N. Schuch, QIP, Lecture Notes of the 44th IFF Spring School 2013; J. I Cirac and F. Verstraete, J. Phys. A: Math. Theor. **42**, 504004 (2009); F. Verstraete, J. I. Cirac and V. Murg,

- Adv. Phys. **57**, 143 (2008).
- [15] E. Mascarenhas, H. Flayac, and V. Savona, Phys. Rev. A **92**, 022116 (2015); J. Cui, J. I. Cirac, and M. C. Bañuls, Phys. Rev. Lett. **114**, 220601 (2015).
- [16] J. J. Mendoza-Arenas *et al*, Phys. Rev. A **93**, 023821 (2016).
- [17] M. Zwolak and G. Vidal, Phys. Rev. Lett. **93**, 207205 (2004).
- [18] I. P. McCulloch, arXiv:0804.2509.
- [19] G. Vidal, Phys. Rev. Lett. **91**, 147902 (2003); G. Vidal, Phys. Rev. Lett. **939**, 040502 (2004).
- [20] G. de las Cuevas *et al*, New J. Phys. **15**, 123021 (2013).
- [21] F. Verstraete and J. I. Cirac, cond-mat/0407066.
- [22] J. Jordan *et al*, Phys. Rev. Lett. **101**, 250602 (2008).
- [23] H. C. Jiang, Z. Y. Weng and T. Xiang, Phys. Rev. Lett. **101**, 090603 (2008).
- [24] R. J. Baxter, Physica A **106**, pp18-27 (1981); R. J. Baxter, Exactly Solved Models in Statistical Mechanics, Academic Press, London, (1982); R. J. Baxter, J. Math. Phys. **9**, 650 (1968); R.J. Baxter, J. Stat. Phys. **19** 461 (1978); T. Nishino and K. Okunishi, J. Phys. Soc. Jpn. **65** pp. 891-894 (1996); T. Nishino and K. Okunishi, J. Phys. Soc. Jp. **66**, 3040 (1997); R. Orús and G. Vidal, Phys. Rev. B **80**, 094403 (2009); R. Orús, Phys. Rev. B **85**, 205117 (2012).
- [25] Ho N. Phien *et al*, Phys. Rev. B **92**, 035142 (2015); P. Corboz *et al*, Phys. Rev. B **94**, 155123 (2016); P. Corboz, Phys. Rev. B **94**, 035133 (2016); M. Levin, and C. P. Nave, Phys. Rev. Lett. **99**, 120601 (2007); Z. Y. Xie *et al*, Phys. Rev. Lett. **103**, 160601 (2009); H. H. Zhao *et al*, Phys. Rev. B **81**, 174411 (2010); Z. Y. Xie *et al*, Phys. Rev. B **86**, 045139 (2012); G. Evenbly and G. Vidal, Phys. Rev. Lett. **115**, 180405 (2015); G. Vidal, Phys. Rev. Lett. **98**, 070201 (2007); R. Orús and G. Vidal, Phys. Rev. B **78**, 155117 (2008).
- [26] A. A. Gangat, T. I and Y.-Jer Kao, arXiv:1608.06028.
- [27] S. R. White, Phys. Rev. Lett. **69**, 28632866 (1992); S. R. White, Phys. Rev. B **48**, 10345 (1992); U. Schollwöck, Rev. Mod. Phys. **77**, 259 (2005); U. Schollwöck, Annals of Physics **326**, 96 (2011).
- [28] F. Letscher *et al*, arXiv:1611.00627.
- [29] N. Malossi *et al*, Phys. Rev. Lett. **113**, 023006 (2014).
- [30] Tony E. Lee, H. Häfner and M. C. Cross, Phys. Rev. A **84**, 031402 (2011).
- [31] M. Marcuzzi *et al*, Phys. Rev. Lett. **113**, 210401 (2014).
- [32] M. F. Maghrebi and A. V. Gorshkov, Phys. Rev. B **93**, 014307 (2016).
- [33] M. Hönig *et al*, Phys. Rev. A **90**, 021603 (2014).
- [34] M. Hönig *et al*, Phys. Rev. A **87**, 023401 (2013).
- [35] A. Lucia *et al*, Phys. Rev. A **91**, 040302 (2015); F. G. S. L. Brandao *et al*, J. Math. Phys. **56**, 102202 (2015).
- [36] Intuitively, $|a\rangle\langle b| \simeq |a\rangle \otimes |b\rangle$.
- [37] This was, in fact, the approach taken in Ref.[17] for finite-size 1d systems, using Matrix Product Operators (MPO) [18] to describe the 1d reduced density matrix, and proceeding as in the Time-Evolving Block Decimation (TEBD) algorithm for ground states of 1d local Hamiltonians [19].
- [38] Such a construction does not guarantee the positivity of the reduced density matrix [20]. However, we shall see later that this lack of exact positivity is not too problematic in our numerical simulations.
- [39] Regarding settings where dissipation is not so strong, our algorithm is a good starting point to compute steady states in the strong-dissipation regime. The strength of the dissipation can then be lowered down adiabatically, and using as initial state the one pre-computed for slightly-stronger dissipation. In this way one may get rid of local minima and obtain good results also in the weak dissipation regime.
- [40] Other approaches [25] would also be equally valid here.
- [41] Notice that, as such, Δ is *not* the typical expectation value of an operator for the reduced density matrix ρ (which would look like $\text{tr}(O\rho)$, with O the operator at hand), but rather the expectation value of the vectorized Liouvillian \mathcal{L}_\sharp on the vectorized density matrix $|\rho_s\rangle_\sharp$. In practice, we saw that the imaginary part of Δ is negligible, $\text{Im}(\Delta) \sim 10^{-15}$.
- [42] As a word of caution: notice that Δ and ϵ_n can be used to benchmark our calculations, but they do not characterize the distance to the steady state.
- [43] To have an idea of how efficient this is, let us imagine the following alternative strategy to compute the steady state $|\rho\rangle_\sharp$: instead of considering operator \mathcal{L}_\sharp , we consider the Hermitian and positive semidefinite operator $\mathcal{L}_\sharp^\dagger\mathcal{L}_\sharp$, and target $|\rho\rangle_\sharp$ as its ground state. This ground state could be computed, e.g., by an imaginary time evolution. The problem, however, is that the crossed products in $\mathcal{L}_\sharp^\dagger\mathcal{L}_\sharp$ are non-local, and therefore the usual algorithms for time evolution are difficult to implement unless one introduces extra approximations in the range of the crossed terms [26]. Another option is to approximate the ground state variationally, e.g., via the Density Matrix Renormalization Group [27] or similar approaches [15] in 1d, or variational PEPS in 2d [21]. In the thermodynamic limit, however, this approach does not look very promising because of the non-locality of $\mathcal{L}_\sharp^\dagger\mathcal{L}_\sharp$ mentioned before. In any case, one could always represent this operator as a PEPO (in 2d), which would simplify some of the calculations, but at the cost of introducing a very large bond dimension in the representation of $\mathcal{L}_\sharp^\dagger\mathcal{L}_\sharp$. For instance, if a typical PEPO bond dimension for \mathcal{L}_\sharp is ~ 4 , then for $\mathcal{L}_\sharp^\dagger\mathcal{L}_\sharp$ it is ~ 16 . This large bond dimension may be manageable in 1d, but in 2d it implies *extremely* slow calculations for practical purposes. Another option would be to target the variational minimization of the real part for the expectation value of \mathcal{L} [15]. This option, however, is also dangerous in 2d because of the presence of many local minima. Additionally, the correct norm to perform all these optimizations is the one-norm of $\mathcal{L}(\rho)$ which, in contrast to the more usual 2-norm, is a hard figure of merit to optimize with variational TN methods. The use of real-time evolution is thus a safer choice in the context of the approximation of 2d steady states.